DTU Library

The long term stability of lidar calibrations

Courtney, Michael; Gayle Nygaard, Nicolai

Publication date:
2014

Document Version
Publisher's PDF, also known as Version of record

DTU Wind Energy

The long term stability of lidar calibrations

Department of Wind Energy I-Report

Michael Courtney[1] and Nicolai Gayle Nygaard[2]

(1) DTU Wind Energy, (2) DONG Energy

DTU Wind Energy E-0033

January 2014

DTU Vindenergi
Institut for Vindenergi

Author (s): Michael Courtney[1] and Nicolai Gayle Nygaard[2]
Title: The long term stability of lidar calibrations
Department: Department of Wind Energy (1)
Collaborating with: DONG Energy (2)

Summary (max 2000 characters):

Wind lidars are now used extensively for wind resource measurements. One of the requirements for the data to be accepted in support of project financing (so-called 'bankability') is to demonstrate the long-term stability of lidar calibrations. Calibration results for six Leosphere WindCube lidars are used examine this stability. Calibration results before and after periods of field service are examined. No evidence of systematic drift is observed but some significant statistical variation is seen. We believe that much of the calibration variation is due to differing environmental parameters pertaining in the different calibration periods. This is supported by sliding-window analyses of one lidar at one location where the same order of variation is observed as between pre-service and post-service calibrations.

DTU Wind Energy E-0033
January 2014

Contract no.:
[Tekst]

Project no.:
[Tekst]

Sponsor:
DONG Energy

Frontpage:
[Tekst]

Pages: 37
Tables: 0
References: 3
ISBN nr.: 978-87-92896-50-6

Technical University of Denmark
Department of Wind Energy
Frederiksborgvej 399
Building 118
4000 Roskilde
Denmark
Telefon +45 2132 7248

www.vindenergi.dtu.dk

Preface

This is the first of two reports in the DONG Energy funded research project 'Bankable lidar' and deals primarily with the stability of calibration results for Leosphere Windcube lidars. The second report will deal with how the calibration results are influenced by shear and turbulence.

The original version of this report (July 2013) has been revised with the addition of pre and post calibration results from a second campaign and some extra analysis concerning the previously reported erratic behaviour of the sensing height error. This second and final version is dated January 2014.

Content

1. Introduction 6
2. Datasets 7
3. Calibrations 9
4. Results from single calibrations 11
5. Sliding window method 26
6. Discussion 30
7. Conclusions 31
8. Recommendations 31

References 31

Appendix A – Plausibility tests at Horns Rev 2 and Østerild 33

Summary

Wind lidars are now used extensively for wind resource measurements. One of the requirements for the data to be accepted in support of project financing (so-called ‘bankability’) is to demonstrate the long-term stability of lidar calibrations. Calibration results for six Leosphere WindCube lidars are used examine this stability. Calibration results before and after periods of field service are examined. No evidence of systematic drift is observed but some significant statistical variation is seen. We believe that much of the calibration variation is due to differing environmental parameters pertaining in the different calibration periods. This is supported by sliding-window analyses of one lidar at one location where the same order of variation is observed as between pre-service and post-service calibrations.

1. Introduction

Wind lidars have great potential to become a cost effective and more flexible alternative to meteorological masts for wind energy resource assessment. Since their commercial introduction 6-7 years ago, the most popular types have sold in numbers exceeding several hundred. The first generation devices that were effectively still prototypes have been replaced by second generation versions that are truly industrial products with much improved reliability. Whereas the early systems had frequent failures, contemporary units are considerably more reliable. Continuous operation without issues for periods of up to 2 years have been observed.
But before LiDARs can be used as stand-alone instruments for resource assessment, their so-called 'bankability' has to be proven. Bankability is a concept that is frequently cited but rarely defined. Ultimately bankability relates to the ability to finance a wind energy project on the basis of the given measurements. In the context of this project we have identified the following requirements:

1. An accredited LiDAR calibration procedure, where a LiDAR is compared with a trusted reference instrument,
2. Best practices documenting recommended procedures for installation, maintenance and data monitoring of LiDARS.
3. Characterisation of the site sensitivity of particular lidar types,
4. Documentation of the long-term stability of lidar measurements.

Of these 4 points the first two are already fulfilled. DTU have been accredited (by the Danish standards authority DANAK) for wind lidar (WindCube) calibrations since January 2012 and have performed in excess of 40 such calibrations. Calibrations are performed on each unit individually and the applied traceability forms the basis for an uncertainty budget. Secondly, an IEA Recommended Practice [1] was released in March 2013 and has since been downloaded from the IEA web-site over 1300 times.

A resource assessment requires not just a measurement of the wind speed and direction but also an estimate of the measurement uncertainty. Assessing this uncertainty starts with the calibration procedure which allows us to assign an uncertainty to the calibration result in relation to traceable (international) standards. However this is not quite enough since for the actual application the lidar will be used both at a different place and at a later time. Items 3 and 4 on our list of bankability requirements reflect these two issues. Since the lidar will be moved from the calibration site we must understand if and how differences in various environmental variables will affect the lidar results (site sensitivity, point 3). For any meaningful lidar campaign, the measurement duration will be significant, probably at least one year. It is therefore also important to investigate whether the lidar's measurements will retain their accuracy over this period (long-term stability, point 4).

Analysing the site sensitivity can be tackled in two ways. One approach is to perform a 'classification' study where we, treating the lidar device as a black box, attempt to isolate and quantify the sensitivity of the lidar to specific parameters (e.g. temperature, wind shear, turbulence intensity etc.). This is the approach proposed in the new version of IEC 61400-12-1 (Annex L) [2]. The challenge is to deal with the high degree of cross-correlation between the variables (e.g wind shear and turbulence) and also to successfully account for the sensitivity of the reference instruments themselves. Work on this method is underway although the results are not yet completely convincing.

A second approach is, in contrast to regarding the lidar as a black box, to recognise the physics pertaining to the measurement process and in so doing, attempt to deduce the sensitivities to specific parameters. This is the method we will adopt in the current project where we will specifically look at the influence of turbulence and wind shear. This work will be reported in a subsequent report.

This report will concentrate on examining the long-term stability of wind lidars.

Method

In the investigation presented here we use six separate LiDAR units, each of which has undergone repeated calibration campaigns at the Høvsøre test station. For most of the units the separation between the first and the latest calibration campaign is more than two years. Between the repeated calibrations, each unit has been deployed either onshore or offshore in the vicinity of a mast equipped with cup anemometers.

To address the long-term stability of the calibration results we compare the results of the different calibration tests for each LiDAR unit and quantify the differences in the calibration parameters to demonstrate that any drift in the LiDAR performance is within the uncertainty of the reference instruments. In addition, for the field campaigns we conduct a plausibility test by comparing the lidar measurements to those of an on-site meteorological mast or a wind speed derived from turbine SCADA data. The purpose of this plausibility test is to support the temporal stability of the LiDAR calibration.

We also test the short-term repeatability of the lidar calibration for a single unit by sequencing the time series of a calibration campaign into several near-concurrent sub series. The calibration analysis is then performed independently on each sub series and the results are compared.

2. Datasets

For this study we had access to calibration data from six different lidars. All lidars were WindCubes manufactured by Leosphere. Five of six units were version 1 of the WindCube, while the last lidar was a V2. The V1 and V2 versions of the WindCube measure using essentially the same technology and scan patterns, the main difference being in how the beam is physically positioned. We believe therefore that the results from the V1 are to a large degree applicable to the V2 although due to more consistent manufacturing procedures, we expect a greater degree of uniformity between different V2 units. The WindCube is a pulsed lidar system, and we expect the main conclusions in this report to be applicable to pulsed lidar systems in general.

All lidars were calibrated at the Høvsøre test station following the DANAK accredited calibration protocol (see below). For each lidar we have two or three distinct calibration campaigns separated by either an onshore or offshore deployment for wind resource assessment or service by the manufacturer. This is indicated in the time line in Figure 1.

As part of the Bankable Lidar project WindCubes 44 and 103 have been deployed at the Fino-2 offshore met mast. At the conclusion of the measurement campaign both lidars were re-calibrated at Høvsøre.

Figure 2 shows the timespan between consecutive calibrations for each lidar. The longest time between two calibrations is for WindCube 26, which was deployed on an offshore substation for more than two years

.

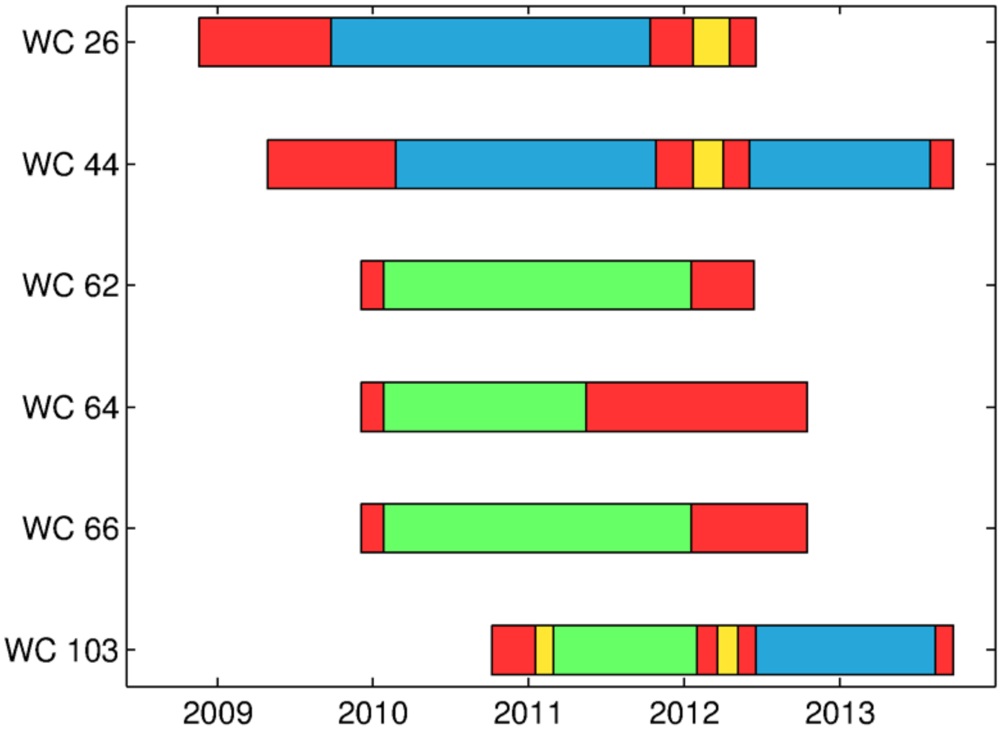

Figure 1 Time line of lidar deployments. Red: calibration at Høvsøre. Yellow: service by lidar manufacturer. Blue: offshore measurement campaign. Green: onshore measurement campaign.

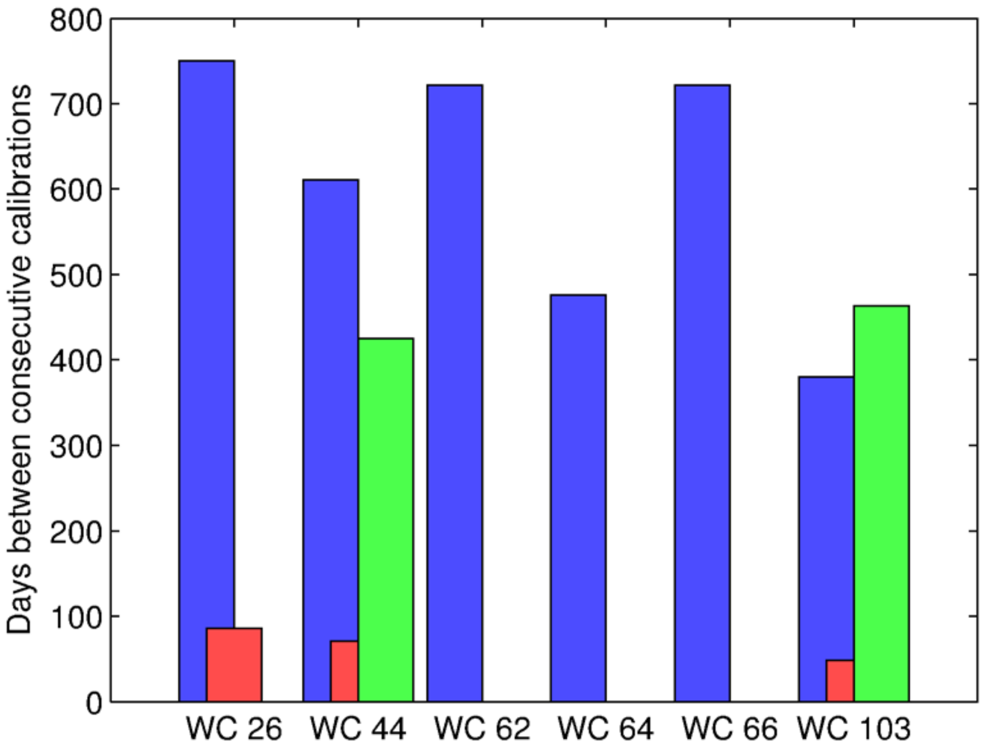

Figure 2 Days between consecutive lidar calibrations. Blue bars give the interval between the first and the second calibration. Red bars (green bars) indicate the separation between the second and third calibration (third and fourth calibration) where applicable.

3. Calibrations

Here we use the word calibration in the sense defined by the International Bureau of Weights and Measures [3]. In this context the lidar wind speed measurement is compared with a reference instrument, which in our case is a cup anemometer mounted on a met mast. By linear regression the transfer function between the two is established.

The calibrations are carried out at the Høvsøre test station by DTU, following a DANAK accredited procedure. The calibration measurements use the 116.5 m mast at Høvsøre. Lidar wind speed measurements at 40 m, 60 m, 80 m, 100 m, and 116.5 m are compared with cup anemometer wind speeds at the same heights. The mast has wind vanes at 60 m, 80 m, and at 100 m. At 40 m and 116.5 m the wind direction measured at 60 m and 100 m are used, respectively.

3.1 Cup calibrations

Care has been taken to ensure that systematic differences between cup calibrations do not significantly effects the results. This is necessary since cup anemometers calibrated in different wind tunnels are known to give results that differ by up to 1%. Even for cups calibrated in the same wind tunnel, changes in practice or instrumentation can also give significant differences. We have normalised all cup anemometer calibration results to remove these effects by calculating the average ratios between the calibration results from various cups performed in the different wind tunnels.

3.2 Filters

A series of four filters is applied to eliminate data where the lidar or the mast is in wake, the wind speed is outside the calibration range of the cup anemometers, the lidar data has poor signal to noise ratio, or there is risk of icing affecting the cup anemometers. At each height the measurements are considered valid provided:

1. Wind direction is between 230° and 300°
2. The 10-minute wind speed of the reference instrument in the range 4-16 m/s
3. The availability of the WindCube is 100%
4. The temperature measured at the 2 m and 100 m levels on the mast are above 2°C

If any of the conditions are not met the data point is discarded.

According to the DANAK scheme a calibration is considered complete once 600 valid data points valid have been accumulated at each measurement height after filtering. In addition, 150 valid 10 minute wind speeds in the range 8-16 m/s are required at the 40 m level after filtering, as well as 150 valid points in the range 4-8 m/s at 116.5 m.

3.3 Linear regression

Based on the data remaining after filtering the transfer function between the cup anemometer wind speed and the lidar wind speed is found at each heights using linear regression analysis. Three regression models are used

1. Free linear regression applying the model $y = kx + C$, which relates the lidar wind speed y to the reference wind speed x. A gain k different from one indicates a wind speed dependent lidar error, while a non-zero offset C is a systematic bias in the lidar measurement
2. Forced linear regression $y = mx$ with no offset
3. Three-parametric regression applying the model $y = k_u u + k_{\sigma_w} \sigma_w + k_g g + D$ for the lidar wind speed. Here u is the reference wind speed, σ_w is the standard deviation of the vertical wind speed measured by the lidar, and g is the local gradient of the wind speed profile at the considered height. The latter is estimated by fitting the cup anemometer wind speed at all heights with the profile $u(z) = a + bz + cz^2 + dz^3 + e\ln(z)$, where z is the height in meters. The wind speed gradient at measurement height z_0 is then given by $g(z_0) = b + 2cz_0 + 3dz_0^2 + e/z_0$.

In each case the regression parameters and their 95% confidence intervals are tabulated along with the corresponding R^2 values.

In this report we do not consider the comparison between the lidar wind direction and that recorded by the wind vanes on the mast.

3.4 Uncertainty budget

The lidar uncertainty is evaluated as a combination of terms calculated as binned averages in 0.5 m/s wind speed bins centred on integer multiples of 0.5 m/s in the range 4-16 m/s. A separate uncertainty of the lidar measurement is found at each height.

Under the assumption of independent contribution to the lidar uncertainty it can be stated as

$$u_{\text{lidar}} = \sqrt{u_{\text{ref}}^2 + \Delta v^2 + \frac{\sigma_{\text{lidar}}^2}{n} + \sigma_{\text{dev}}^2}$$

The individual components are

- u_{ref}: the standard uncertainty of the reference instrument
- Δv: the mean lidar deviation, meaning the bin averaged difference between the lidar wind speed and the reference wind speed
- $\sigma_{\text{lidar}}/\sqrt{n}$: the uncertainty of the lidar mean wind speed. The standard deviation of the lidar wind speed in a bin is σ_{lidar} and n is the number of samples in the bin
- σ_{dev}: the standard deviation of the lidar wind speed deviation (lidar wind speed minus reference wind speed) in the bin, corresponding to the statistical uncertainty of the lidar measurements

4. Results from single calibrations

For each of the datasets we have performed linear regressions on the complete dataset having first applied the filtering described in section 3.2. In each case all of the three error models described in section 3.3 have been applied. Thus we have results for free and forced linear regressions as well as the 3p error model.

Key results from these analyses are shown in the following sections (4.1 and 4.3) in the form of scatter plots of the value from the second (post service) calibration versus the value from the first (pre service) calibration (for example Figure 3). Each point represents a pair of values for one lidar and one height. With 6 lidars and 5 different heights we have a total of 30 points in each plot. For perfect agreement between the second and first calibrations, all the points would lie on the line y=x. Any drifting of the lidar or lack of repeatability in the calibration procedure will cause deviation from this ideal correlation.

For the free and forced regression results we have attempted to identify whether the correlation between the first and second calibrations varies significantly for specific lidars or for specific heights. The differences between the various gains and offsets are grouped according to height and lidar number in the plots of section 4.2.

All the results examined are for the speed calibration. We have not attempted to examine drift in the direction since the large offset uncertainty in both the lidar and the reference wind vanes does not make such an analysis meaningful.

4.1 Scatter plots free and forced regression results

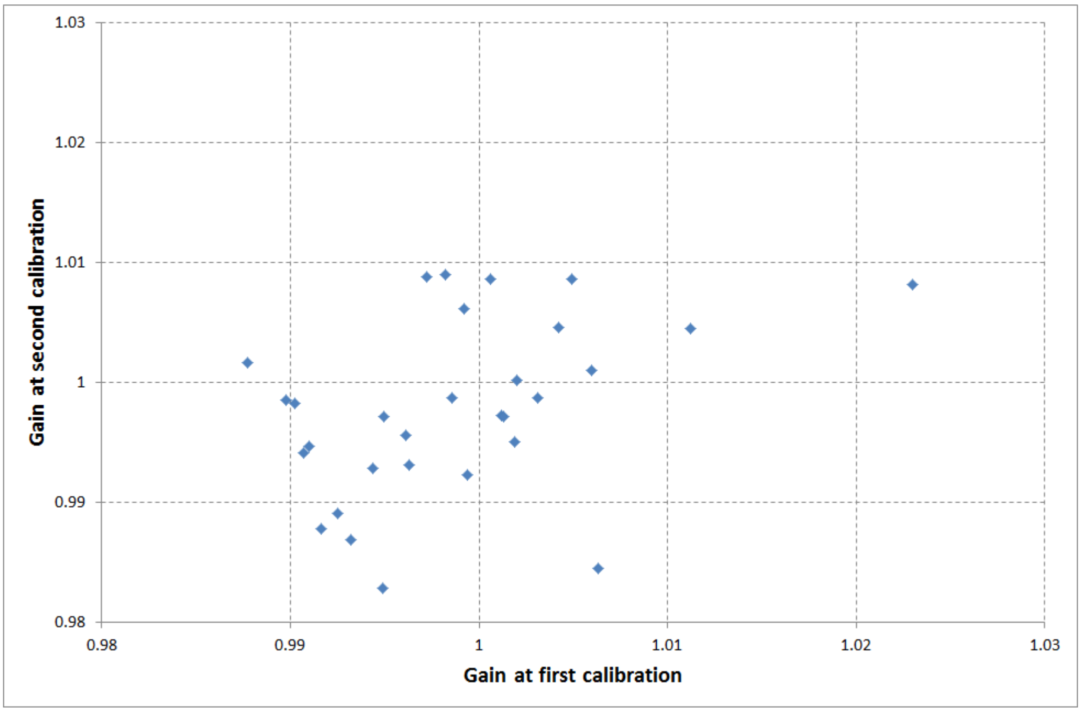

Figure 3 Scatter plot of free gain (k). Value from the second calibration vs value from the first calibration.

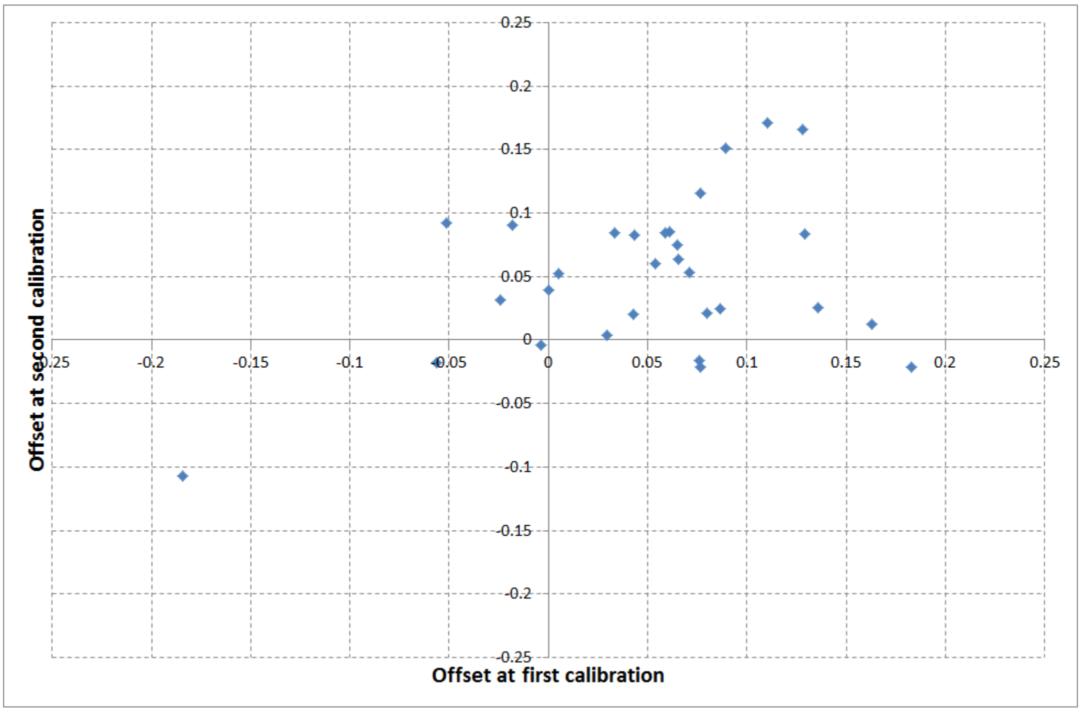

Figure 4 Scatter plot of offset (C). Value from the second calibration vs value from first calibration.

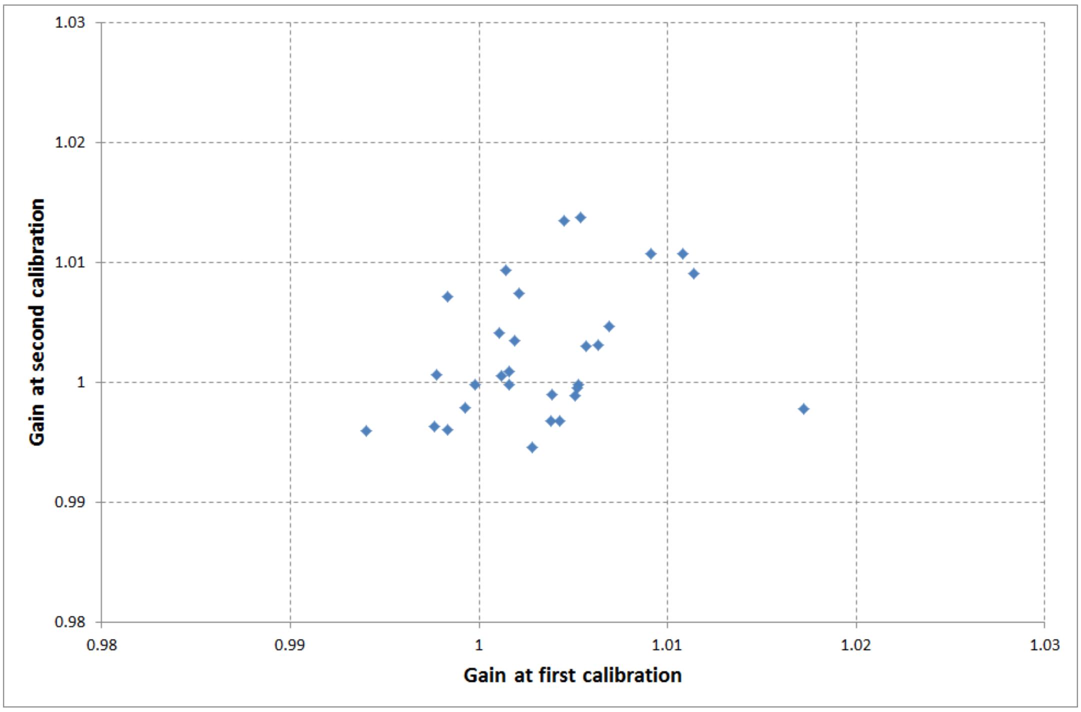

Figure 5 Scatter plot of forced gain. Value from the second calibration versus value from the first calibration.

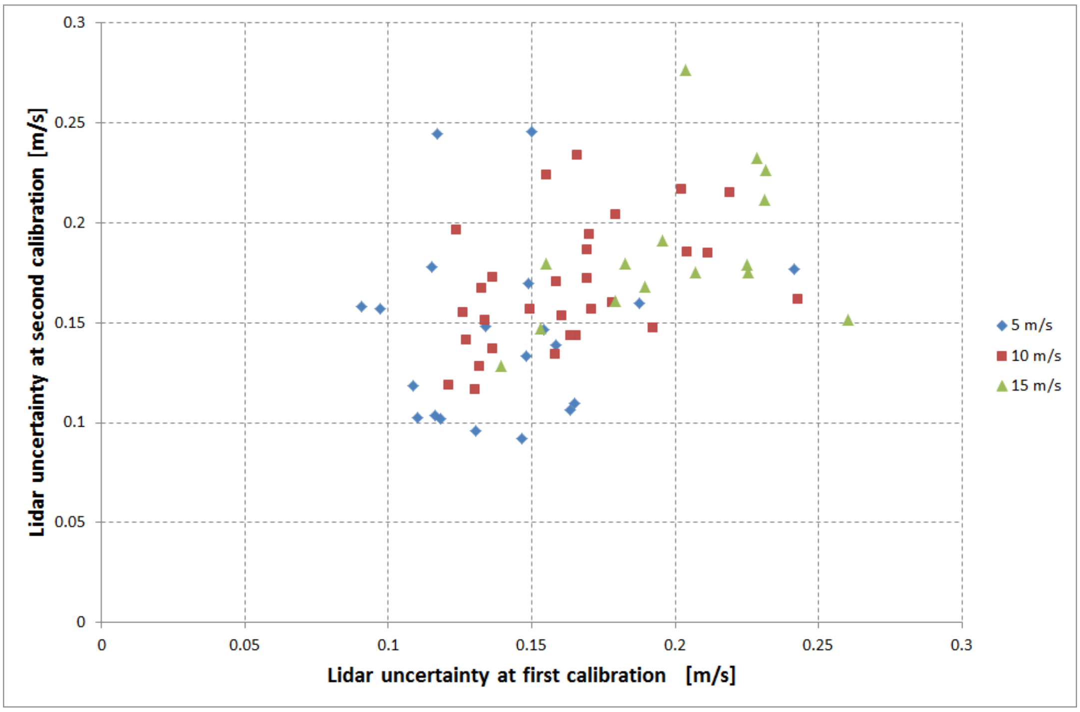

Figure 6 Scatter plot of lidar uncertainty including mean offset (unc_lidar1) at three different wind speeds (5 m/s blue, 10 m/s brown and 15 m/s green). Values from the second calibration versus values from the first calibration.

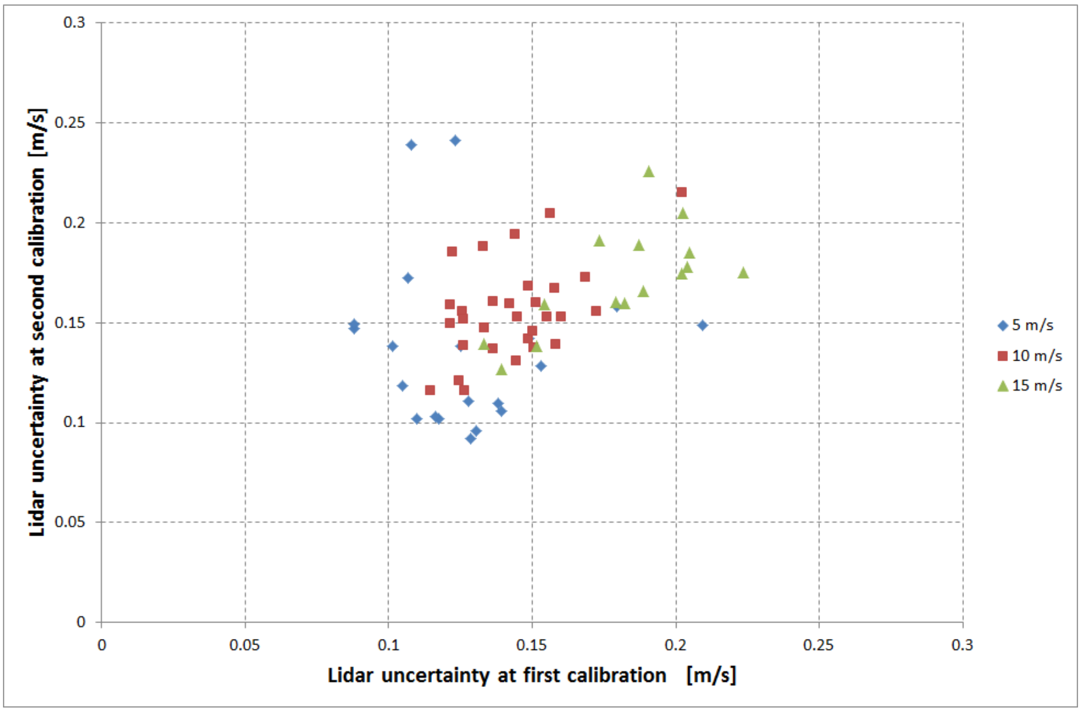

Figure 7 Scatter plot of lidar uncertainty not including mean offset (unc_lidar2) at three different wind speeds (5 m/s blue, 10 m/s brown and 15 m/s green). Values from the second calibration versus values from the first calibration.

4.2 Grouped differences of free and forced regression results

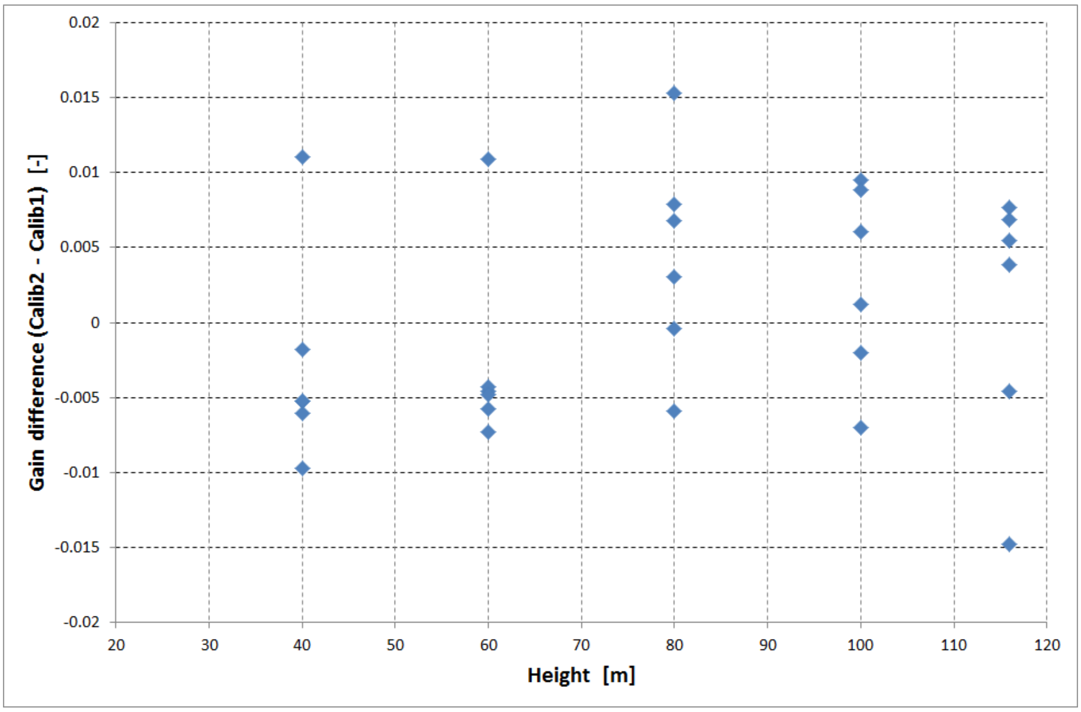

Figure 8 Difference in free gain (k) between the first and second calibrations grouped by measuring height. Note that the gain scale is absolute and should be multiplied by 100 to get the percentage change.

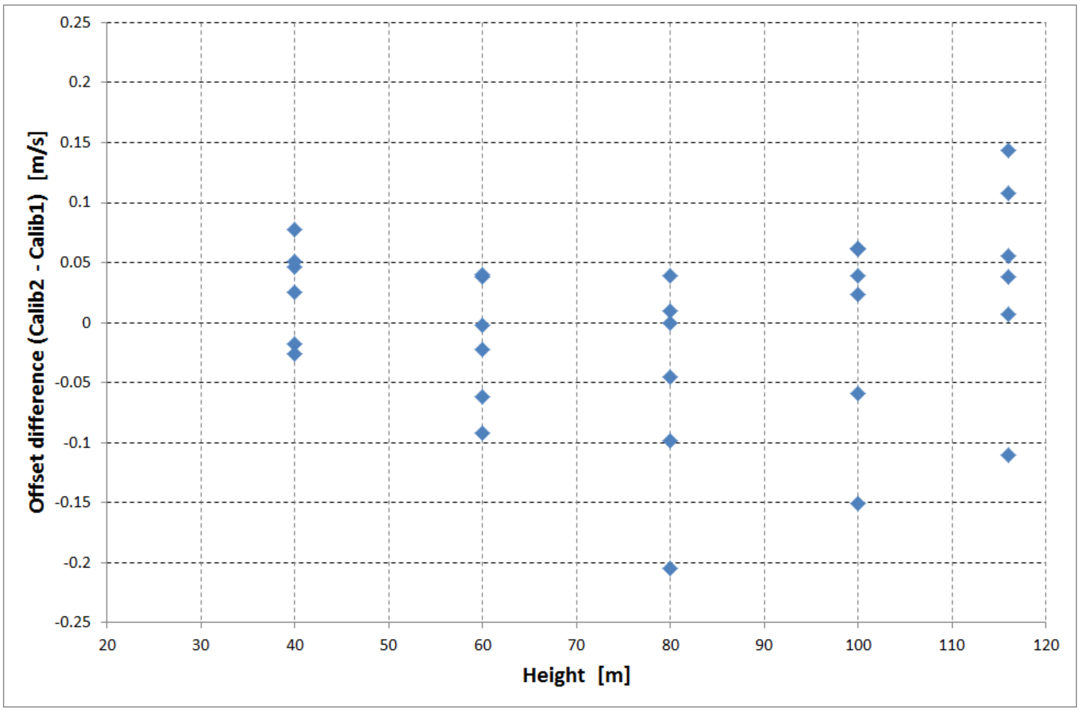

Figure 9 Difference in offset (C) between the first and second calibrations grouped by measuring height.

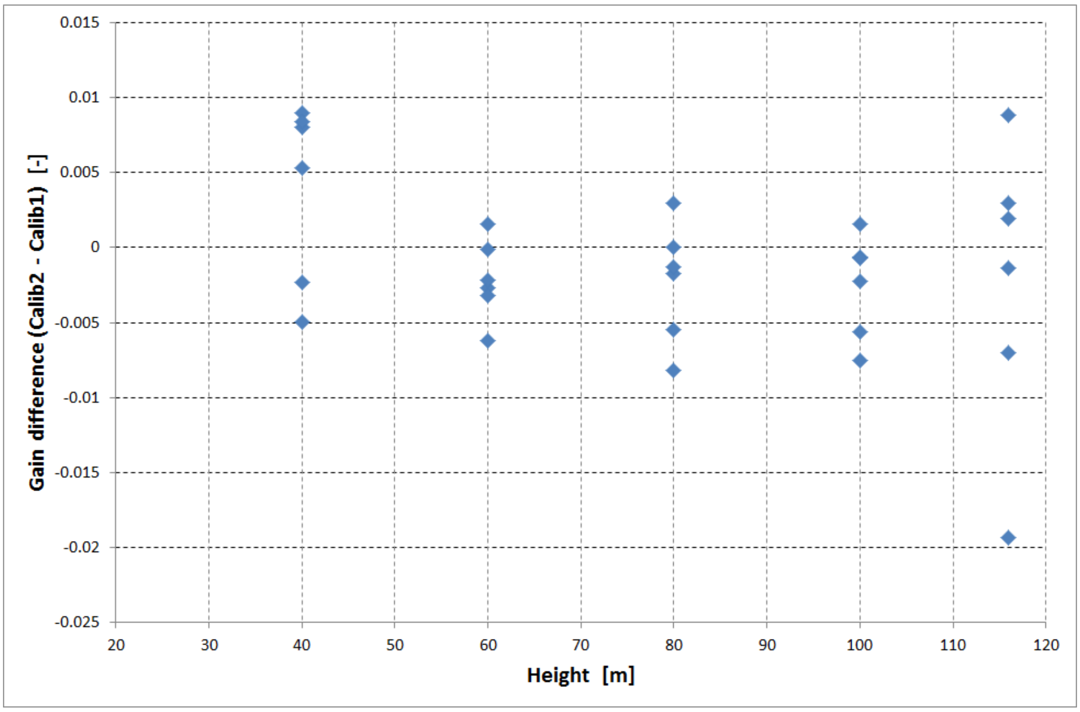

Figure 10 Difference in forced gain (M) between the first and second calibrations grouped by measuring height. Note that the gain scale is absolute and should be multiplied by 100 to get the percentage change.

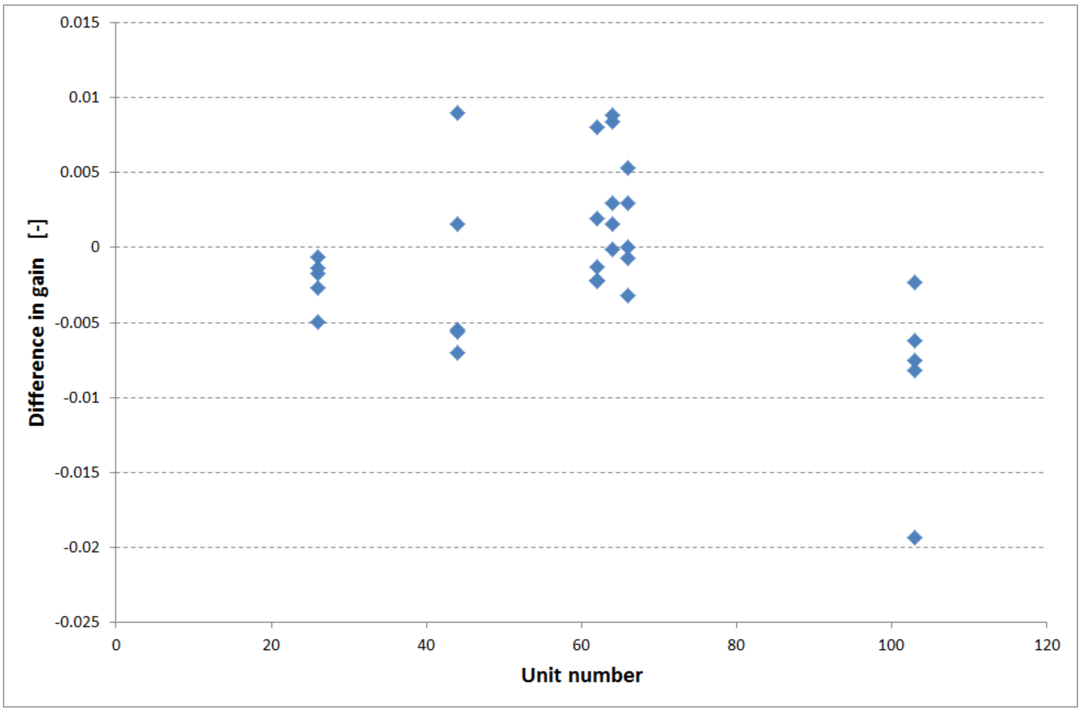

Figure 11 Difference in forced gain (M) between the first and second calibrations grouped by lidar unit number. Newer lidars are indicated by higher unit numbers.

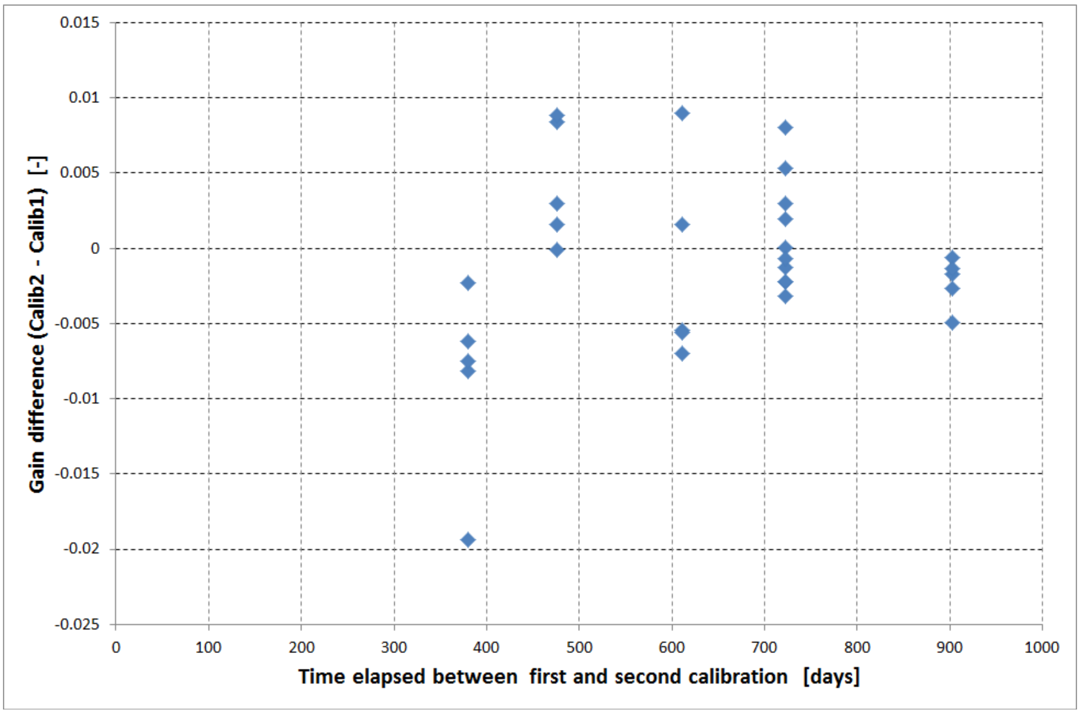

Figure 12 Difference in forced gain (M) between the first and second calibrations grouped by elapsed time between the two calibrations. Note that two lidars have exactly the same elapsed time - hence there are only 5 distinct groups.

4.3 Analysis of the 3p regression results

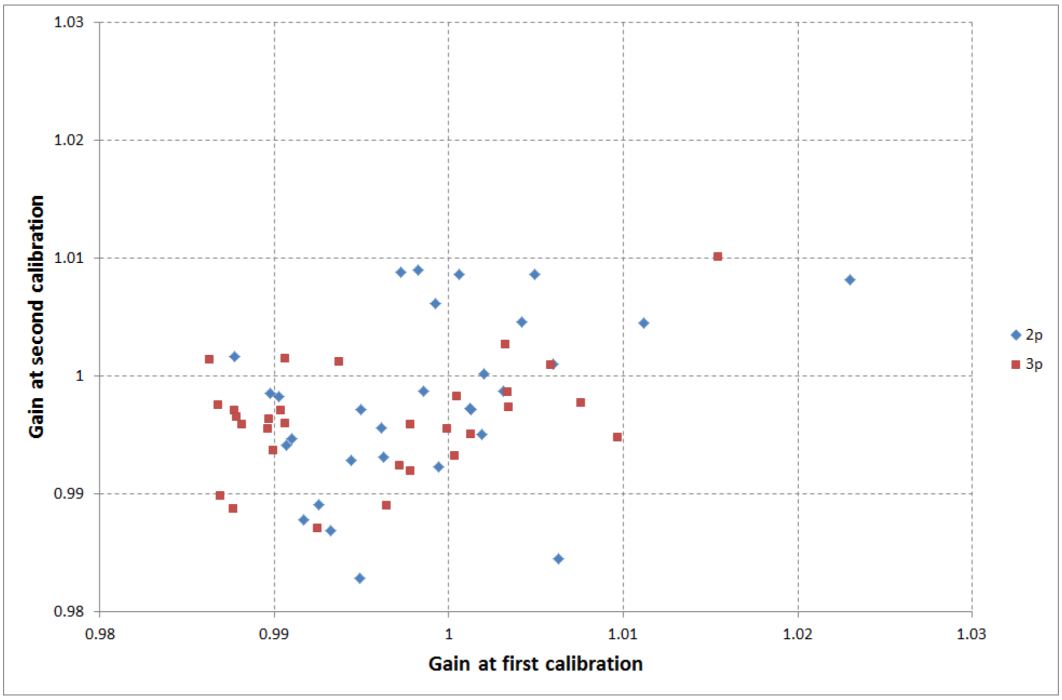

Figure 13 Scatter plot of speed gain from the 3p regression (brown) with the value for the 2p regression also shown (blue).

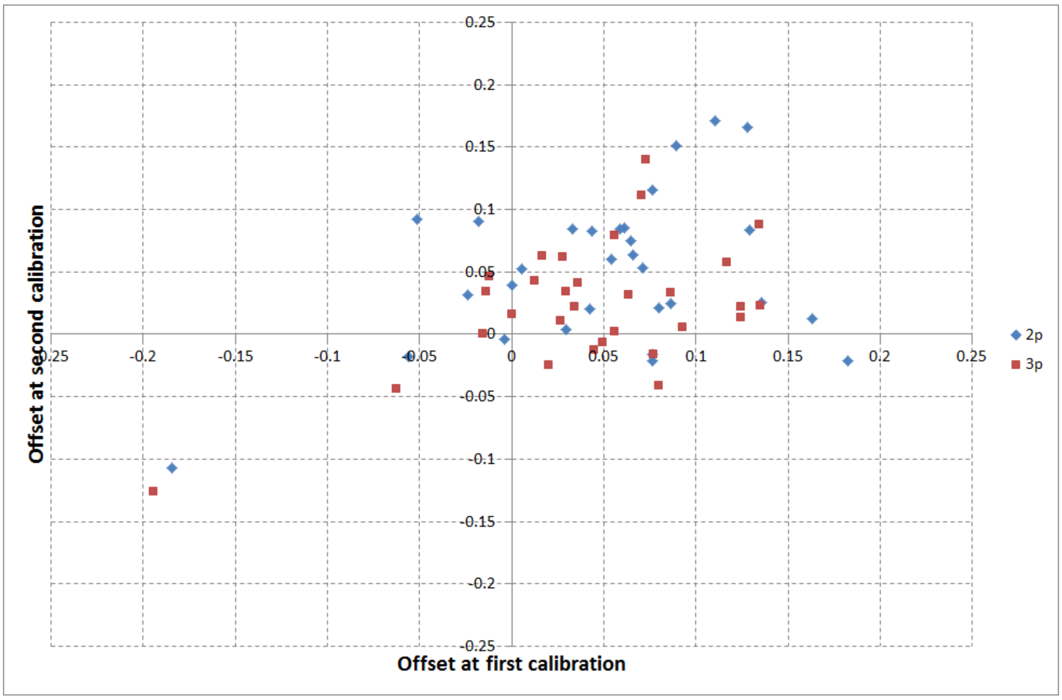

Figure 14 Scatter plot of offset from the 3p regression (brown) with the value for the 2p regression also shown (blue). Values from the second calibration vs values from the first calibration.

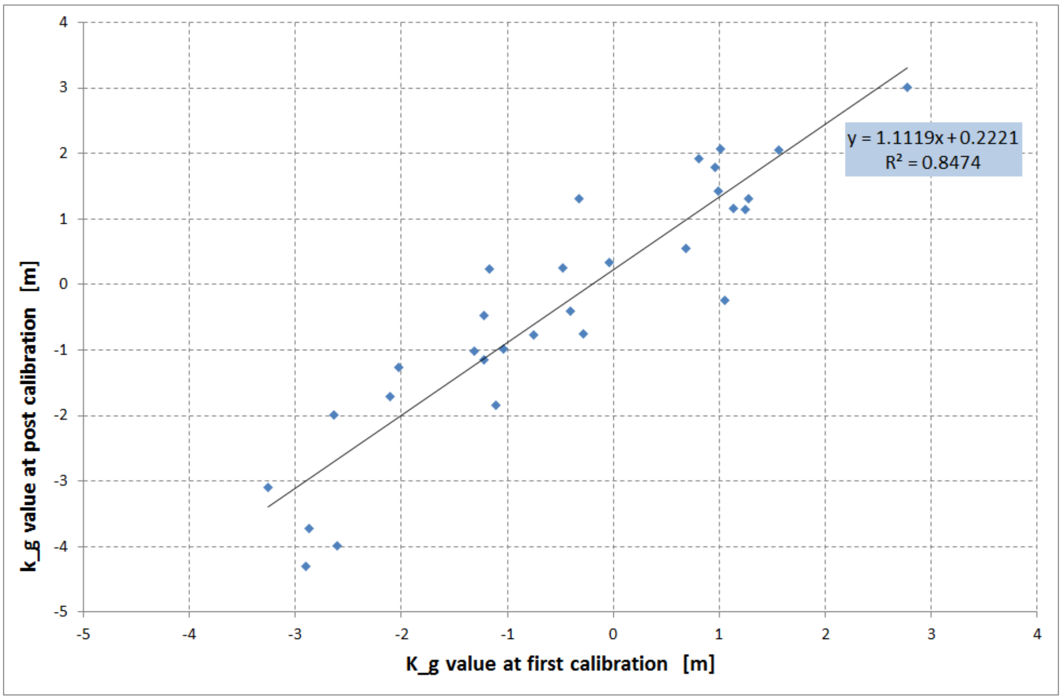

Figure 15 Scatter plot of sensing height error (k_g) from the 3p regression. Values from the second calibration vs values from the first calibration.

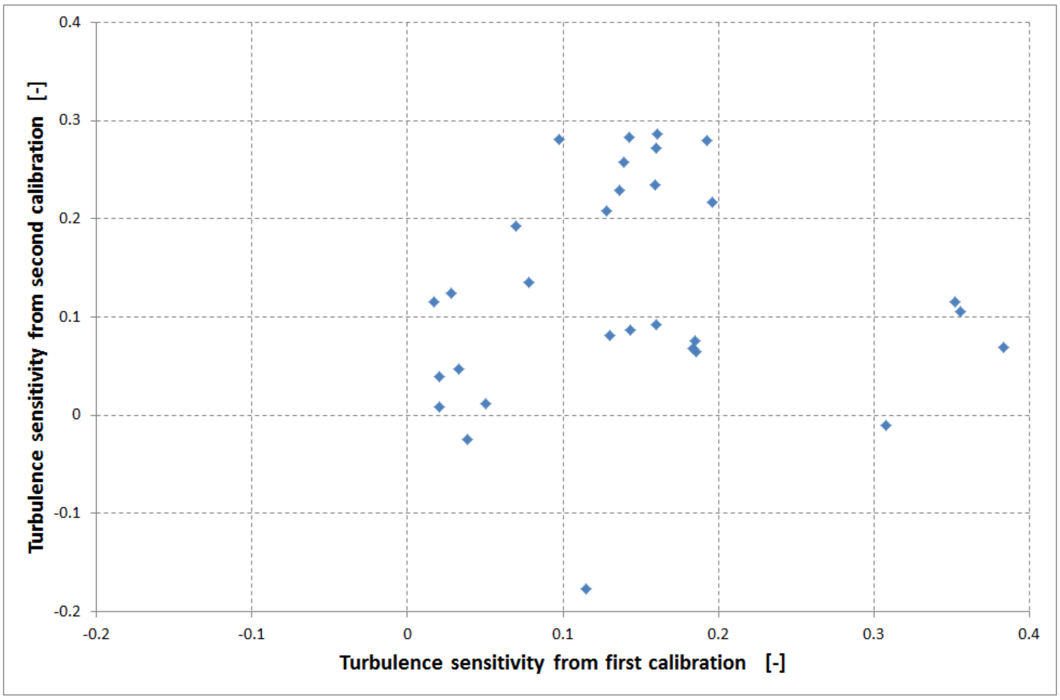

Figure 16 Scatter plot of turbulence sensitivity (k_sigma_w) from the 3p regression. Values from the second calibration vs values from the first calibration.

4.4 Discussion of the regression results

Our mission is to ascertain whether lidar calibrations are stable over time. Choosing the simplest error model, the forced linear regression, we can gain an impression of the calibration variability by studying just one parameter. Thus Figure 5 is the first plot to examine. Here in Figure 17 we have repeated Figure 5 but also inserted limits representing calibration differences of ±1%. It can be seen that for all but one pair of results, the first and calibrations lie within 1% of each other. The distribution of the gain differences is also shown in Figure 18 where it can be seen that a significant proportion of the differences lie well within ±1%. The mean of the distribution is -0.001, the standard deviation 0.006.

Looking at the results from the free regression model we must bear in mind that the gain and offset parameters are not entirely independent. For this reason we can see a larger scatter in the free gain parameter (Figure 3) than for the forced gain. The corresponding results for the offset (Figure 4) show a rather large scatter and rather weak correlation between the values for the first and second calibrations.

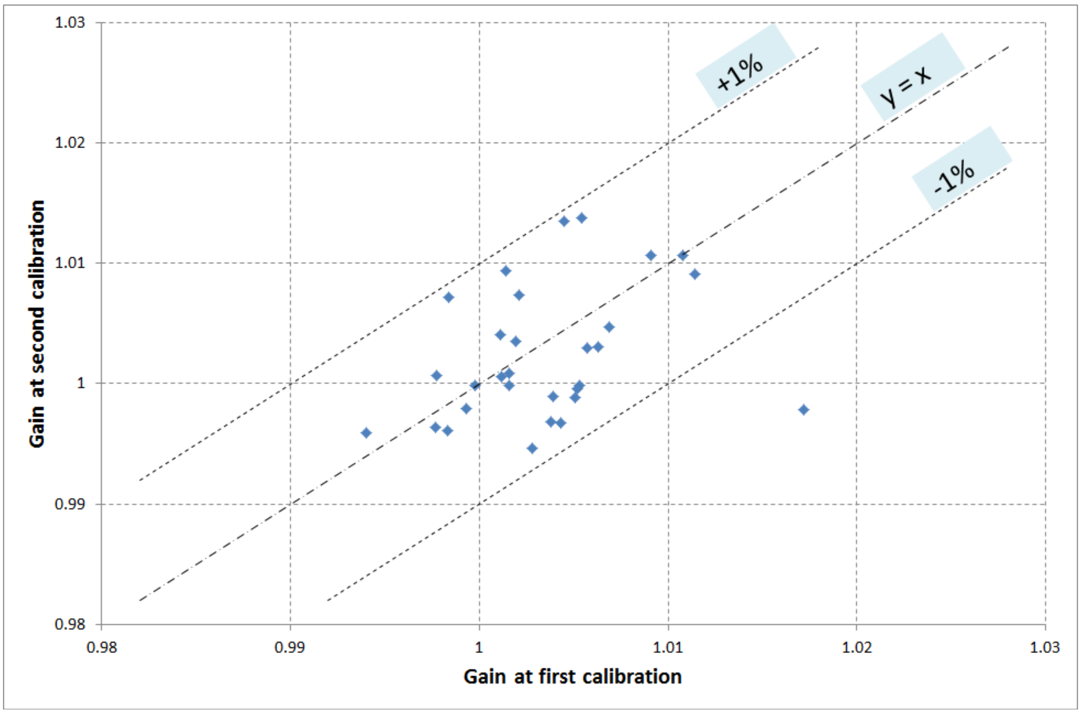

Figure 17 Scatter plot of forced gain with +-1% error limits inserted.

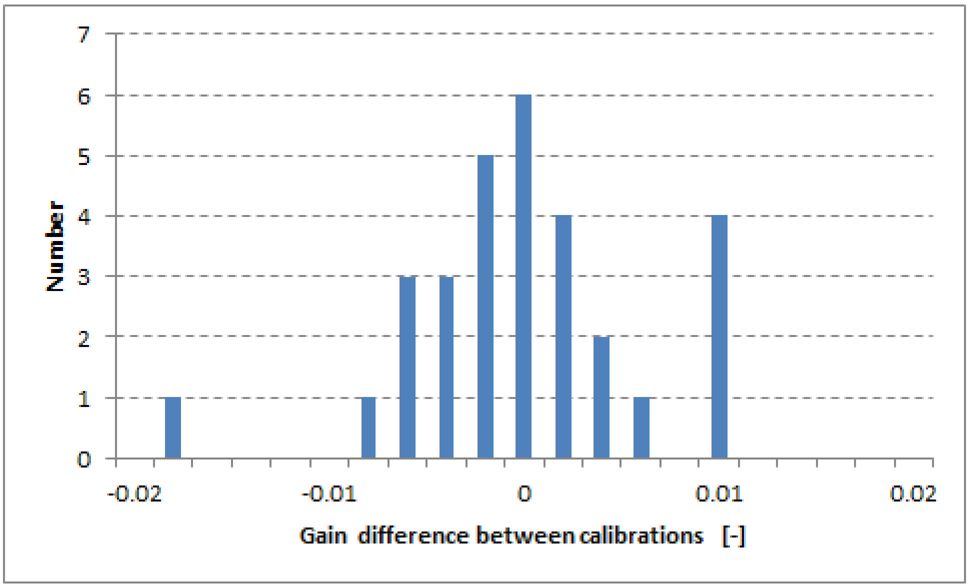

Figure 18 Distribution of gain difference between pre and post calibrations (absolute scale). Multiply x axis values by 100 to represent the difference as a percentage.

The uncertainties calculated from the first and second calibration results are compared in Figure 6 (including the mean offset) and Figure 7 (not including the mean offset, in the case that the calibration expression is used to correct the lidar wind speeds) for three different wind speeds (5, 10 and 15 m/s). We can see no significant and persistent difference between the uncertainty of the first and second calibrations. Some correlation between the values for the first and second calibration is apparent. The absolute uncertainty as expressed in these plots (in m/s) increases with wind speed.

In Section 4.2 we have attempted to identify whether the magnitude of the calibration differences are specifically linked to specific heights (Figure 8, Figure 9 and Figure 10), specific lidars (Figure 11) or to the elapsed time between the calibrations (Figure 12). Grouping by height shows no convincing systematic differences although for the forced gain the largest deviations between calibrations is observed for the highest height 116m for which the reference wind speed is derived from a top mounted anemometer.

The differences displayed by different lidars (Figure 11) vary quite considerably. We cannot of course conclude from this that the differences are due to the lidars. It could equally be a consequence of the particular conditions during the testing. Smaller differences between calibrations could be indicative of closer similarity of conditions between the two tests.

Finally the calibration differences have been grouped by the elapsed time between first and second calibration (Figure 12). Since the elapsed time is related to each individual lidar, the data are similar to Figure 11 but presented in a different order. If there was any clear deterioration with time we would expect to see increasing differences with time. In fact we see that the smallest differences are actually for the lidar that was the longest time in service. Figure 12 seems to be our best evidence that the wind speed accuracy of lidars does not appear to significantly degrade with time.

In Section 4.3 we have compared the results from the 3p regression model from the first and second calibrations. Here the error model is extended to include a sensing height error (k_g) and a term to represent the over-speeding effect of turbulence (k_sigma_w). Firstly as can be seen in Figure 13, the speed gain (k_u) derived from the 3p model (brown points) shows a spread similar to those for the free speed gain (blue points) although several of the more extreme differences in the 1p free speed gain are removed. A similar pattern can be seen for the offset (Figure 14) where there is once more a small improvement in using the 3p model. The slightly reduced spread for the more sophisticated 3p regression model can be explained by the ability of this model to correctly assign speed differences to e.g. sensing height error rather than have all errors absorbed in the gain parameter.

Two contrasting results can be seen for the two added parameters – sensing height error (k_g) and turbulence sensitivity (k_sigma_w). The scatter plot of the results for the sensing height error derived from the first and second calibrations Figure 15 shows very good correlation between the two values indicating that this is a persistent and reproducible parameter. Figure 19 shows the distribution of the differences. The mean difference is 0.17m and the standard deviation is 0.76m.

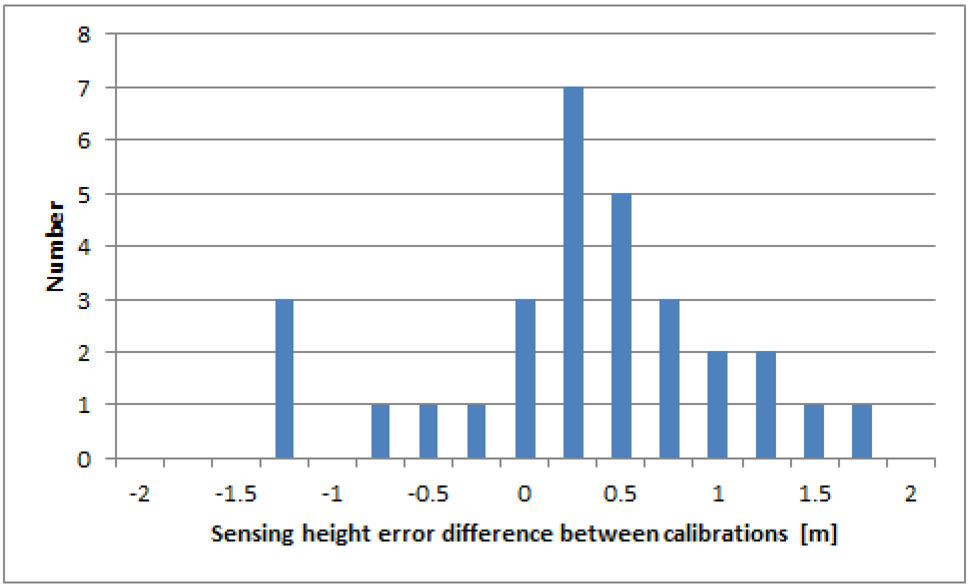

Figure 19 Distribution of sensing height error difference between the first and second calibrations.

In contrast Figure 16 shows that the values for the turbulence sensitivity (k_sigma_w) for the first and second calibration are essentially uncorrelated. This parameter does not seem to capture the influence of the turbulence in a consistent and reproducible manner.

4.5 Update after 2nd field campaign

Following the initial calibration, field service and post-calibration cycle, two of the tested lidars have been used in a second field campaign, followed again by a post-calibration. This gives us the opportunity to perform a second comparison between pre and post calibrations. Unit 44 (V1) and unit 103 (V2) have both been deployed offshore on the Fino-2 platform for a period of close to 12 months. Prior to deployment but after a manufacturers service, both instruments were pre-calibrated (calibration number 3). Immediately after service, both units have been returned to Høvsøre for a post-calibration (calibration number 4). Unfortunately the post-calibration of unit 44 at 40m height proved to be invalid due to periodic obfuscation of the beam by a boom. This has only affected the results at 40m only. We thus have 9 pairs (5+4) of calibrations to compare. These have been inserted in the previous scatter plot of forced gain values. The 9 new values are shown in red, the 25 old values shown in blue in Figure 20.

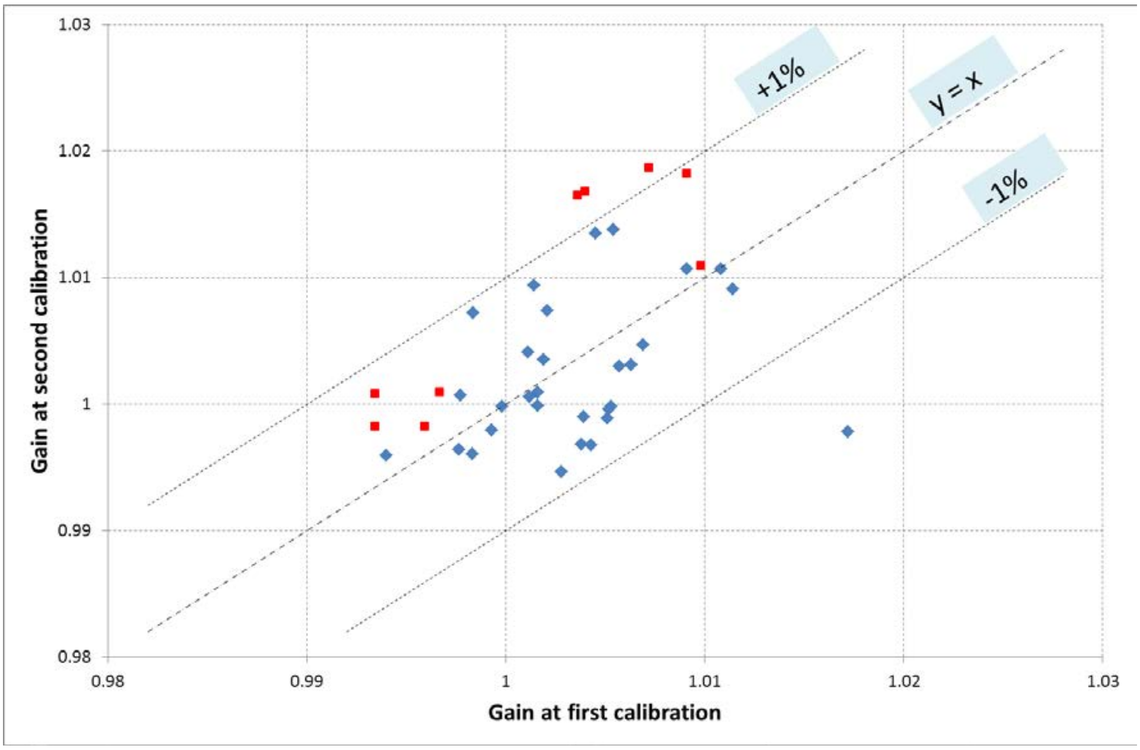

Figure 20 Scatter plot of pre and post forced gain results revised after the second field campaign. The blue triangles are for the first campaign (as before) and the red squares are for the values before and after the Fino platform campaign.

Although three of the nine new values lay slightly outside of the ±1% boundaries, the general conclusion is underlined – that values repeat themselves within about ±1%.

4.6 Time series of calibration results

For WC 44 and WC 103 we now have four individual calibration results spread over a considerable time. In Figure 21 values of offset, free gain and forced gain are plotted as a time series for each of the lidars. The typical variation is again well illustrated but there is no evidence of systematic drifting.

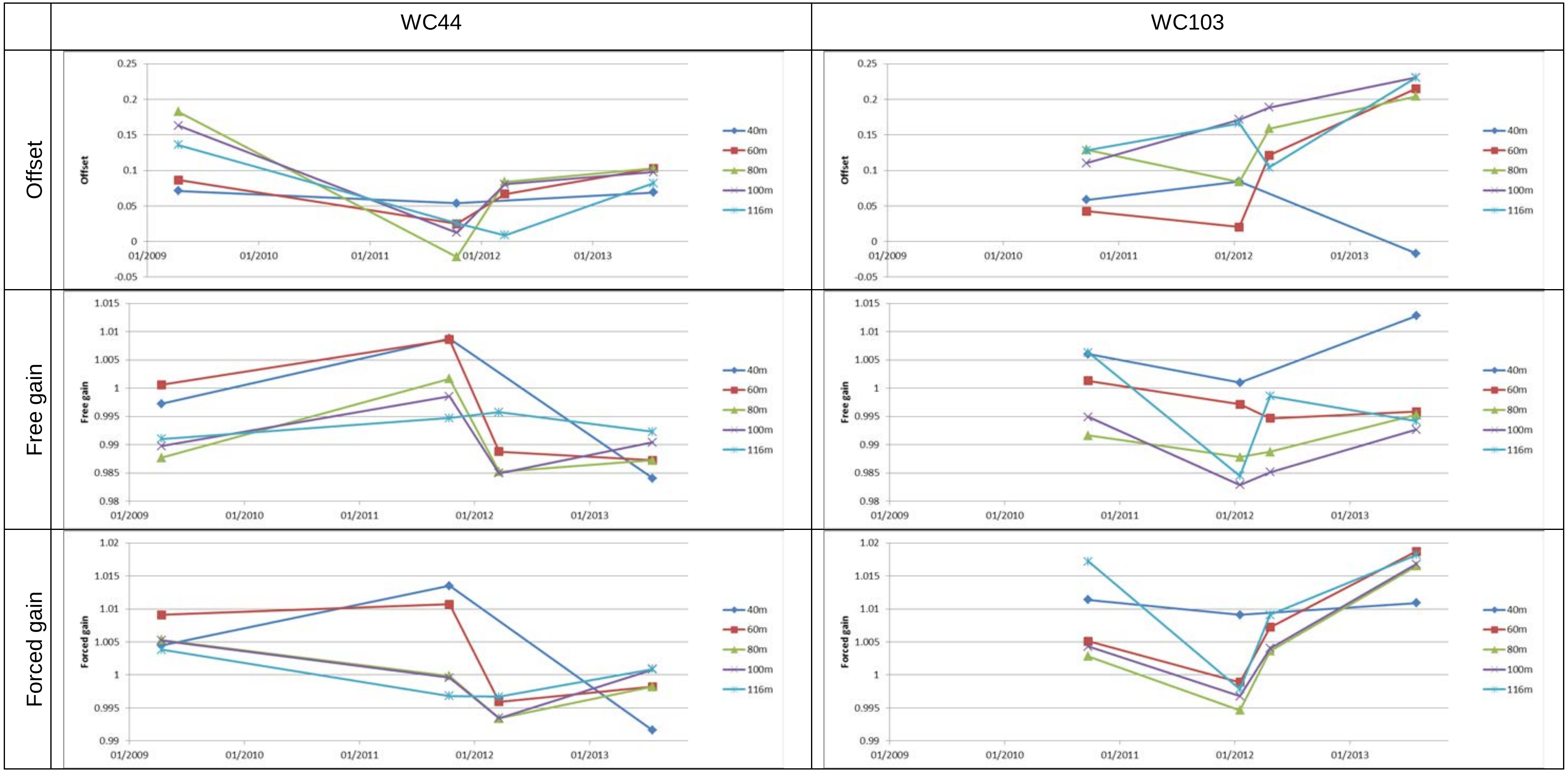

Figure 21 Time series of calibration constants for WC44 and WC103.

5. Sliding window method

The results of Section 4 indicate a significant variation in results between the first and second calibrations. For the forced gain the standard deviation of the difference was 0.6%. In this section we will investigate to what extent this difference can be explained by the sensitivity of the calibration method to external parameters (such as turbulence and shear) rather than real changes in the performance of the lidar over time.

5.1 The concept

Instead of examining the result of just one calibration, the sliding window method performs a whole series of calibrations from a dataset of considerable duration but for one lidar at one location. Each individual calibration should completely fulfil the requirements of the calibration procedure. The dataset is first filtered according to Section 3.2 and from the remaining points the first sub-dataset just fulfilling the population requirements (Section 3.2) is identified. Using this sub-dataset the regression analyses are performed and a calibration result set is duly obtained. Returning to the full dataset, the first point is discarded, the next sub-dataset just fulfilling the population requirements is identified and a result set is calculated for this sub-dataset. The process continues – essentially a window sliding through the dataset although in order to fulfil the distribution requirements the sub datasets will vary in length. Each result set represents a valid calibration result for a calibration starting at that particular time.

5.2 Results

Assuming the lidar performance remains unchanged, the resulting time series of calibration results will reveal how much the ‘natural’ variability of the calibration procedure is. We have selected one period in which three identical lidars were all being calibrated at the same place. For two of the lidars the total period is from January 2012 to September 2012 whilst the third started at the same time but only runs until May 2012.For the two longer series, the total number of individual calibrations is close to 9000. The results are for one height (60m) only. A routine cup anemometer change was made on the 1 June 2012 at this height.

We have chosen to present the following parameters:

Figure	Parameter	Regression model
Figure 21	Forced gain	1P forced
Figure 22	Free gain	1P free
Figure 23	Speed gain	3P free
Figure 24	Offset	1P free
Figure 25	Offset	3P
Figure 26	Sensing height error	3P
Figure 27	Turbulence sensitivity parameter	3P

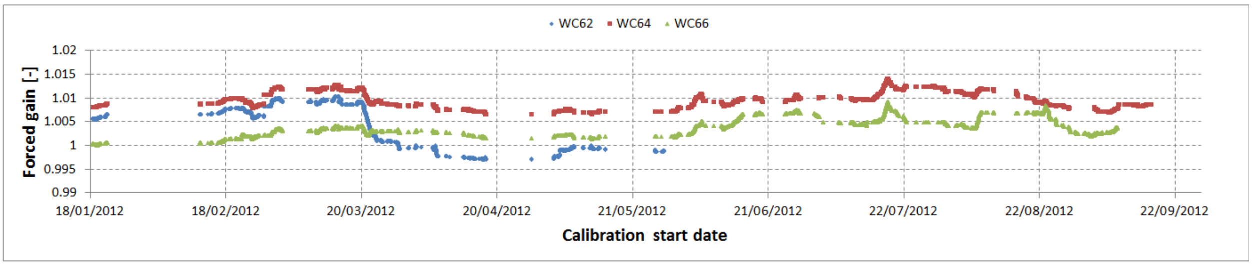

Figure 22 Forced gain sliding window calibration results for three lidars calibrated simultaneously.

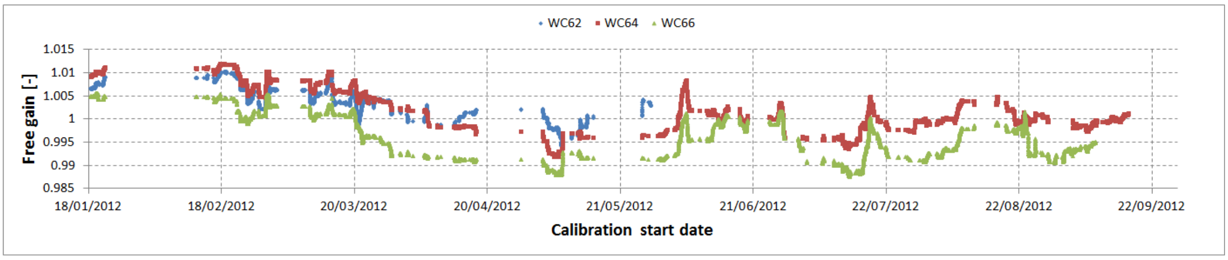

Figure 23 Free gain sliding window calibration results for three lidars calibrated simultaneously.

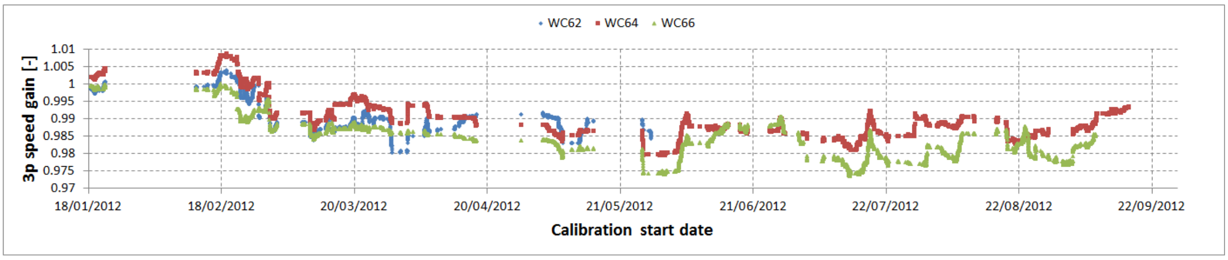

Figure 24 3-Parametric speed gain sliding window calibration results for three lidars calibrated simultaneously.

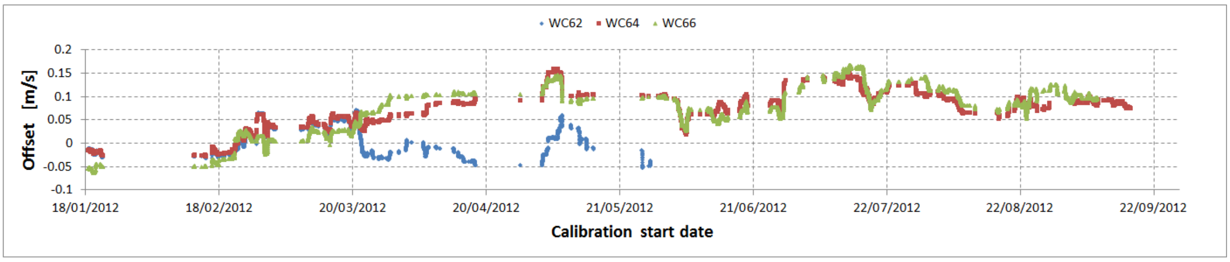

Figure 25 Offset sliding window calibration results for 3 lidars calibrated simultaneously.

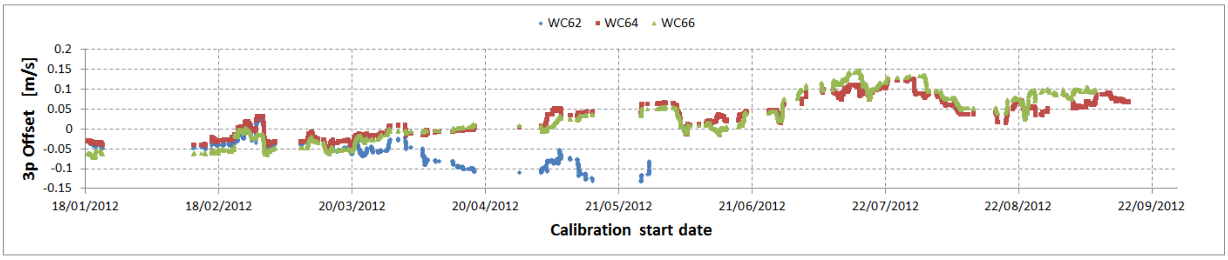

Figure 26 3-Parametric offset sliding window calibration results for 3 lidars calibrated simultaneously.

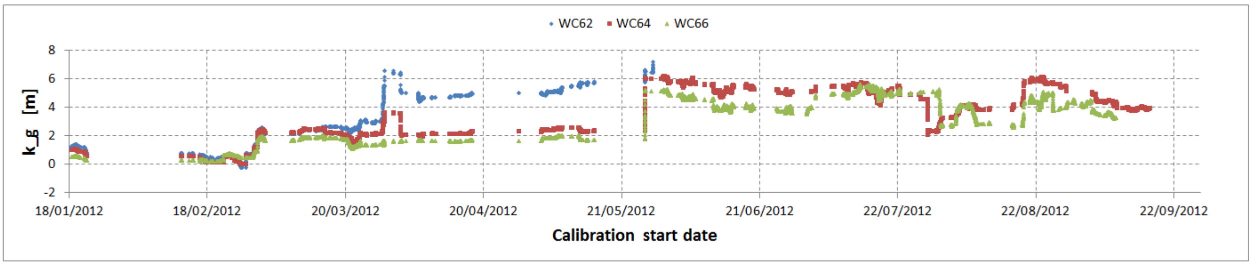

Figure 27 3-Sensing height error (k_g) sliding window calibration results for 3 lidars calibrated simultaneously.

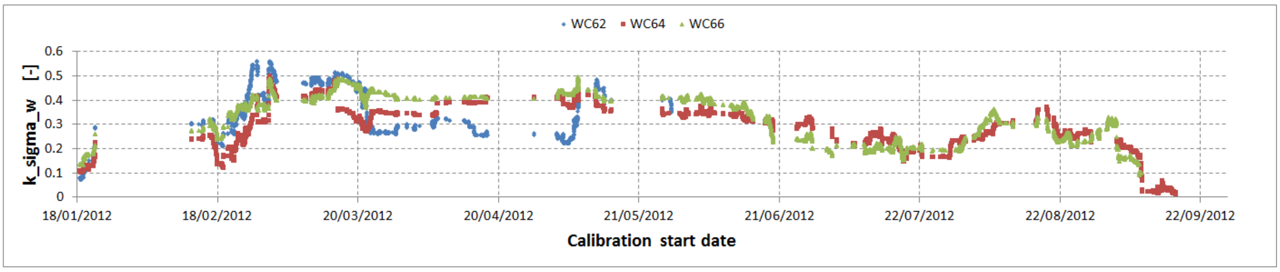

Figure 28 Turbulence sensitivity parameter (k_sigma_w) sliding window calibration results for 3 lidars calibrated simultaneously.

5.3 Discussion of the sliding window results

Once again the results for the forced gain (Figure 21) are the easiest to interpret and can most directly be related to actual lidar accuracy. To start with, all 3 lidars track each other quite well but display individual gain values (based on exactly the same reference wind speed data) that vary by about 1%. Around the 20th March 2012, WC62 suddenly deviates and over the space of a few days its gain value falls by about 1% relative to the other two lidars. The other two lidars continue to track each other well throughout the remainder of the period. There are several observations to be made from this:

1. Most of the variations in calibration results are generic to a lidar type, i.e the lidars generally track each other. The reason for the variation is almost certainly environmental and having approximately the same effect on each of the lidars.
2. At Høvsøre and with our current procedure, this variation is typically within a band of about 1%.
3. As demonstrated by WC62, individual lidar performance can apparently also be degraded significantly although seemingly plausible results are reported.

The variation in the results for the free gain (Figure 22) are larger than for the forced gain but once more WC64 and WC66 track each well over the whole period. WC62 again exhibits deviant behaviour from around the 20th March. Similar behaviour is displayed by the speed gain for the 3p regression (Figure 23) although some rather abrupt changes in value are also observed.

Sliding window results for the offset (Figure 24) and for the 3p offset (Figure 25) also track each other well for the two apparently well-functioning lidars (WC64 and WC66).Here an interesting feature is that the offset values for the two lidars not only track well but are also relatively equal in value. Yet again a clear and marked deviation can be seen for WC62 from around 20th March.

The sensing height error also tracks well for the two well-functioning lidars but quite abrupt changes in value can be identified such as occurs towards the end of May 2013. The explanation for these abrupt changes has been found to be related to the distribution of the wind shear within each calibration data set. With the filtering specified until, now there is no requirement or consideration of the distribution of wind shear. Sensing height error (k_g) estimates are derived from the (partial) regression of wind speed error against wind shear. If there are no significant differences in wind shear, for example because most of the data are from predominantly neutral conditions, it is not possible to perform a reliable regression and addition of a few new values can cause almost chaotic changes in the results. This is the behaviour we have seen in Figure 26.

In order to prevent such behaviour and to ensure meaningful results, a condition stipulating an acceptable shear requirement should be added. In Figure 28 we have taken another sliding window series demonstrating the same erratic behaviour (blue points) and have re-calculated the results after adding the criteria that there should be at least 150 points with a shear value beneath 0.15 m/s/m and 150 points with a shear value above 0.15 m/s (brown points). The value of 0.15 m/s/m is chosen as a typical mid-range value for wind shear. As can be seen from the top pane, this condition can require measurement durations of several months in order to be satisfied, for some part of the series, drastically increasing the number of points required for a calibration. It can be seen that the added condition removes the erratic changes but significant and unexplained differences in sensing height error can still be observed.

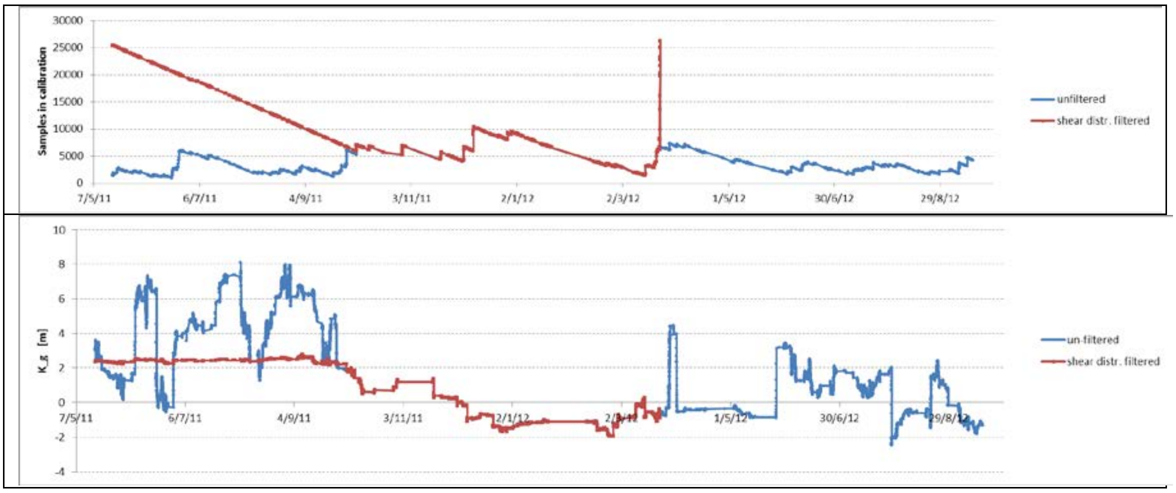

Figure 29 Top - Samples in calibration for the original sliding window series (blue) and for the shear distribution filtered series (brown). Bottom – Sensing height error from sliding window series for the original time series (blue) and for the shear distribution time series (brown).

Results for the turbulence sensitivity parameter (Figure 27) also show good tracking and similar values (for WC64 and WC66) over the entire period. But again it is important to understand why we observe such large changes in value.

6. Discussion

Summing up, what we have learnt from the comparison of individual pre and post calibration results (Section 4) is that the calibrations can vary by about 1%. From studies of a single lidar at a single calibration site (Section 5) we can see that the variability in the calibration results can readily explain this result. We have seen no evidence of systematic deterioration of lidar accuracy over time.

The variability we are seeing for one lidar at one site is none other than an expression of the site sensitivity we discussed in our requirements for bankability in Section 1. If we accept that environmental conditions can be different at different sites it is also reasonable to accept that environmental conditions can vary with time at one site. By gaining a better understanding of the reasons for the variability we can therefore not only improve the repeatability of the lidar calibrations but also reduce the uncertainty we must add when accounting for the differences between calibration and application sites. This is clearly a profitable path of action.

What are the possible reasons for the variation in calibration results that we are seeing? We would like to present several possibilities as a basis for further discussion and work in this area.

1) Shear
    a. The error arising from the (symmetric) sample volume weighting and any non-linear shear.
    b. The error arising from asymmetric sampling volumes and any non-zero shear. Such asymmetry can for example be caused by the convolution of the focusing function and the pulse weighting functions for a pulse lidar.
    c. Non-uniform aerosol distribution in probe volume can cause similar distortions in the weighting of wind speeds from different parts of the probe volume. Mist or cloud for a CW lidar could cause such errors.
    d. Lidar sensing height error and any shear. If the lidar senses at a different height to the reference sensor a discrepancy will be generated that depends on the severity of the shear and the magnitude of the sensing height error.

2) Turbulence - The difference between scalar and vector means depends on the magnitude of the transverse turbulence component(s). Due to very different sampling techniques, cup and lidars will attenuate transverse turbulence differently. There may also be false transverse components due to cross-contamination. Therefore, cup and lidar scalar mean wind speeds will always be different and the difference will vary according to the nature of the turbulence.

3) Reference wind speed sensor sensitivity - Mast mounted cup anemometers are susceptible to flow distortion errors. In additions cup anemometers have sensitivities to turbulence, temperature and tilting angle.

7. Conclusions

Pre and post service calibrations of 6 different wind lidars have been studied in order to ascertain whether lidar accuracy deteriorates with time. No evidence of such deterioration could be found. However, seemingly random variations of up to 1% in speed gain have been observed between the pre and post calibration results. Most of this variation is due to the variability of the calibration procedure itself as demonstrated by sliding window analyses of longer sequences of lidar data.

Several reasons for the lidar calibration variability have been identified. Efforts to reduce this variability will be reported in a subsequent report. It is recognised that some of the variation is due to sensitivity of the reference instruments themselves and this needs further attention.

8. Recommendations

1) Introduce systematic database entry of all calibration results to better be able to study trends and differences in calibration results.
2) Investigate the reasons for the sudden deviation of WC62 as observed in Section 5.3 in an attempt to be able to identify similar events in the future.
3) Add a shear distribution criterion when applying 3p regression to derive sensing height errors.
4) Investigate in depth how shear affects the calibration results. Find the relative importance of the various shear related error sources.
5) Find better methods than the current turbulence sensitivity parameter for accounting for the effects of turbulence on the calibration results. A first effort will concentrate on using vector instead of scalar averaging.
6) Pay even more attention to cup anemometer sensitivity issues, in particular mast effects and the effects of turbulence.

.

References

[1] IEA Wind Expert Group Study On Recommended Practices15. Ground-based Vertically Profiling Remote Sensing For Wind Resource Assessment. Available on-line at http://ieawind.org/index_page_postings/RP/RP%2015_RemoteSensing_1stEd_8March2013.pdf

[2] International Electrotechnical Commission Standard IEC 61400-12-1 rev 2 (CD).

[3] JCGM 200:2008 International vocabulary of metrology

Appendix A – Plausibility tests at Horns Rev 2 and Østerild

In this section we perform a plausibility check on a subset of the lidars during their deployment between the first and the second calibration. The purpose is to support the temporal stability of the lidar calibrations by demonstrating that the units were performing reliably in the period between two calibrations.

WindCube 26 was deployed at the accommodation platform of the Horns Rev 2 offshore wind farm from June 25, 2009 to Aug 19, 2011. The location of the lidar relative to the wind farm is shown in Figure 29. The wind farm consist of 91 Siemens 2.3 MW turbines with a hub height of 68 m and a rotor diameter of 92 m.

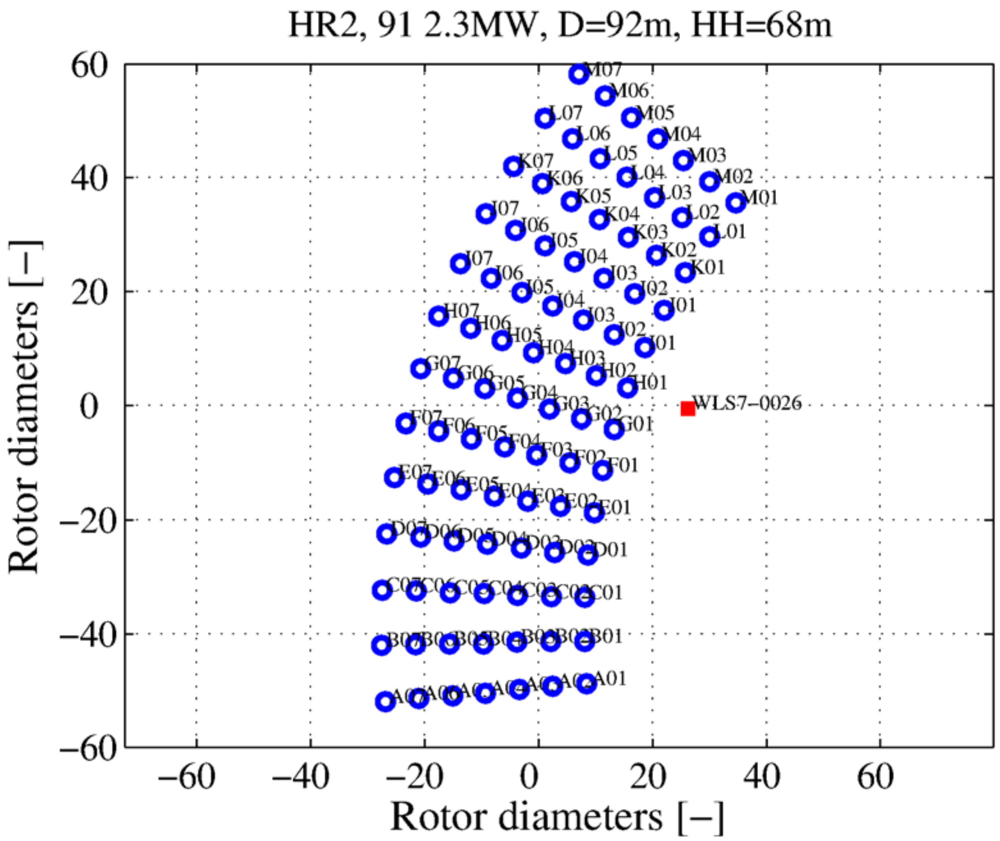

Figure 30 Map of the Horns Rev 2 offshore wind farm. The position of WC26 is indicated by the red square.

The turbine H01 is the one best suited for comparison with the lidar, since it is closest to the accommodation platform. The distance between the lidar and H01 is 1 km, corresponding to 10.9 rotor diameters.

For the purpose of this plausibility test we compare the lidar wind speed measurement 65.75 m with the reading of the nacelle anemometer.

The tiny height difference is not corrected, since nacelle anemometer cannot be considered as reliable as a mast mounted cup, due to the disturbance of the flow around the nacelle and the presence of the rotor blades. It is clear that any comparison between the two instruments can only be indicative.

The data is filtered according to the following criteria:

1. Turbine H01 is fully operational
2. Both the lidar and the nacelle anemometer return a valid wind speed measurement
3. The wind direction recorded by the wind turbine is in the free flow sector [55°,145°], where turbine H01 and the lidar experience the same conditions

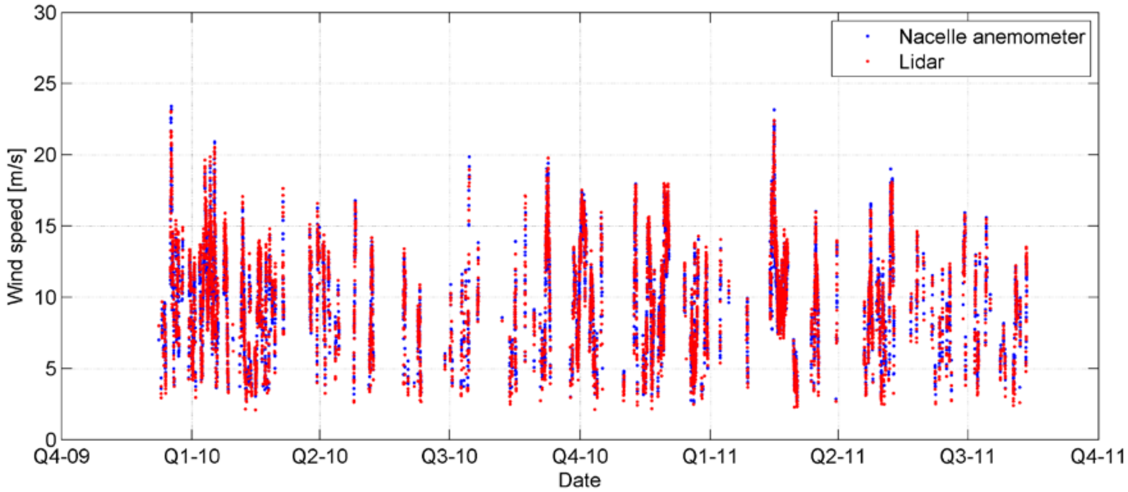

Figure 31 Time series of the wind speed measured by the nacelle anemometer of wind turbine H01 and WC26.

In Figure 30 the time series of the lidar wind speed is compared with that of the nacelle anemometer on H01. We observe a good correlation between the two measurements. This is backed up by Figure 31, which shows the linear regression between the two signals.

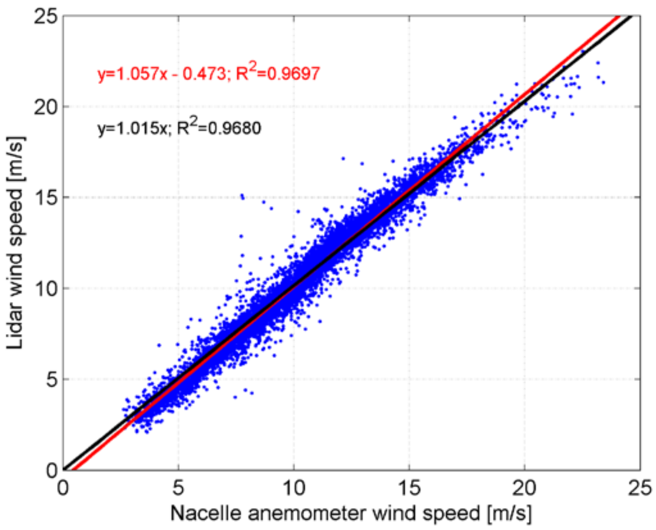

Figure 32 Comparison of the wind speed measured by the nacelle anemometer of wind turbine H01 and WC26.

The scatter is larger than what is generally observed in calibration tests with a met mast. But given the deficiencies of the nacelle anemometer as a reference instrument outlined above and considering the large separation of the two instruments the result demonstrate that the lidar performance was reasonable during the offshore deployment.

Two of the WindCubes were deployed in the vicinity of a 44 m met mast at the Østerild wind turbine test site from April 2010 to September 2011. The results of comparing the lidar wind speed measurement at a single height with that of a cup anemometer mounted on the mast are shown in Figure 32. The data was filtered to exclude periods where the lidar availability was less than 100% and events where the lidar was in the mast shadow.

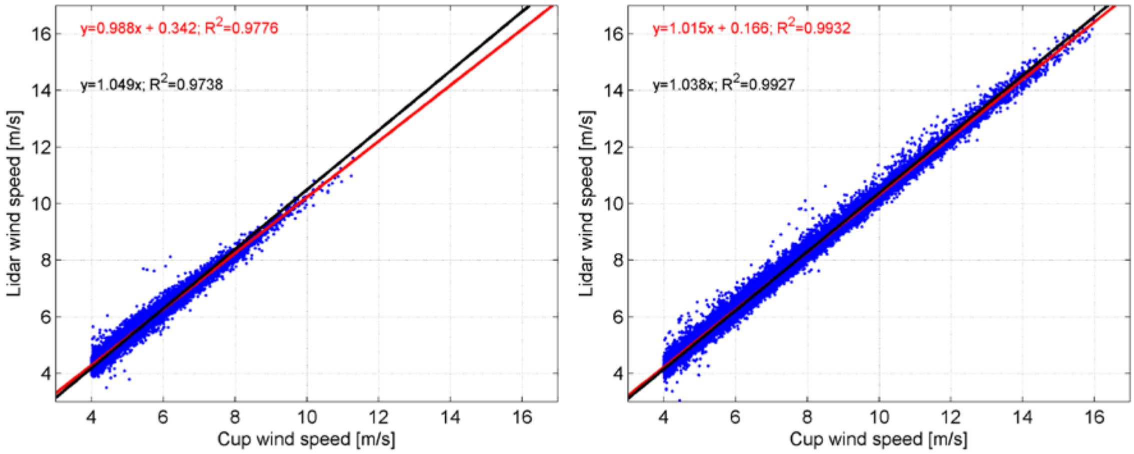

Figure 33 Comparison of the wind speed measured by the two Østerild lidars and the on-site met mast.

Based on this rough analysis the conclusion is that both lidars were plausibly measuring correctly during the field deployment.

DTU Wind Energy is a department of the Technical University of Denmark with a unique integration of research, education, innovation and public/private sector consulting in the field of wind energy. Our activities develop new opportunities and technology for the global and Danish exploitation of wind energy. Research focuses on key technical-scientific fields, which are central for the development, innovation and use of wind energy and provides the basis for advanced education at the education.

We have more than 230 staff members of which approximately 60 are PhD students. Research is conducted within 9 research programmes organized into three main topics: Wind energy systems, Wind turbine technology and Basics for wind energy.

Technical University of Denmark
DTU Vindenergi
Frederiksborgvej 399
Building 118
4000 Roskilde
Denmark
Telefon 46 77 50 85
info@vindenergi.dtu.dk
www.vindenergi.dtu.dk